Journal of Power Sources 195 (2010) 7568–7573

Contents lists available at ScienceDirect

Journal of Power Sources

journal homepage: www.elsevier.com/locate/jpowsour

Performance evaluation of tubular fuel cells fuelled by pulverized graphite

Jong-Pil Kim [a], Ho Lim [a], Chung-Hwan Jeon [a], Young-June Chang [a], Kwang-Nak Koh [b], Soon-Mok Choi [c], Ju-Hun Song [a,*]

[a] School of Mechanical Engineering, Pusan National University (PNU), Busan 609-735, Republic of Korea
[b] College of Nanoscience and Nanotechnology, Pusan National University (PNU), Busan 609-735, Republic of Korea
[c] Korea Institute of Ceramic Engineering Technology (KICET), Seoul 153-801, Republic of Korea

ARTICLE INFO

Article history:
Received 20 January 2010
Received in revised form 13 April 2010
Accepted 26 April 2010
Available online 8 June 2010

Keywords:
Direct carbon fuel cell
Tubular cell
Graphite
Clean coal technology

ABSTRACT

A fuel cell fuelled by carbonaceous graphite is proposed. The tubular fuel cell, with the carbon in a fixed-bed form on the anode side, is employed to convert directly the chemical energy of carbon into electricity. Surface platinum electrodes are coated on the cell electrolyte, which is a yttria-stabilized zirconia (YSZ) tube of 1.5 mm thickness. The effect of using different sizes of graphite powder (in the range 0–180 μm) as fuel is analyzed. Power density and actual open-circuit voltage (OCV) values are measured as the temperature is varied from 0 to 950 °C. The cell provides a maximum power density of 16.8 mW cm^{-2} and an OCV of 1.115 V at the highest temperature condition (950 °C) tested in this study.

1. Introduction

As an energy resource, carbon-loaded coal has many advantages. Coal is not only the most abundant fossil fuel in the world but is also well distributed world-wide. Furthermore, its reserves-to-production ratio stands at about 122 years compared with about 42 years for oil and about 60.4 years for natural gas. Coal is also less expensive than the other resources [1]. Nowadays, most power-plants produce electricity by firing coal. The use of coal, however, raises some problems such as low-efficiency of the heat addition process and emission of pollutants. Therefore, it is necessary to develop clean coal technologies.

Several researchers have developed high-temperature fuel cells fuelled by carbonaceous materials such as coal and biomass [2–5]. A direct carbon fuel cell (DCFC) is one such device that converts chemical energy into electrical energy via an electrochemical process. The advantage of a DCFC with regard to efficiency is derived from the carbon-oxygen reaction ($C + O_2 \rightarrow CO_2$), where complete oxidation of carbon to gaseous carbon dioxide (CO_2) is accomplished with almost no entropy change; this implies that the theoretical efficiency is close to 100% [6–10]. Therefore, the DCFC is potentially one of the most efficient fuel cells under reversible conditions.

DCFCs can generally operate at high temperatures (650–1000 °C) and this offers advantages such as high energy conversion efficiency and the possibility of recycling the exhaust gas for other applications. There are, however, certain disadvantages such as thermal fatigue and stress of the cell materials, as well as sealing under a high temperature [11,12]. Thus, it is important that DCFCs are operated at high temperatures but within a narrow design range.

Efforts in developing DCFC technology have a long history [7,13–15] since the first attempt in 1896 by the American engineer William W. Jacques, who used a cell consisting of a steel pot filled with a molten hydroxide electrolyte at a temperature of 400–500 °C. Since then, molten hydroxide or molten carbonate has been employed as the electrolyte for most DCFCs [15–17]. In such a system, however, there exist problems of electrolyte degradation and the risk of leakage of the liquid.

Recently, DCFCs with solid oxide electrolytes have been developed since these offer simple systems as well as more fuel flexibility [17,18]. Furthermore, tubular fuel cells have more advantages over planar (or button) designs such as an ease in sealing and endurance to thermal stress caused by rapid heating to high temperatures. The present study combines these benefits with the known advantages of using a tubular solid oxide electrolyte for hydrogen applications.

The study proposes a tubular DCFC single cell with a solid oxide electrolyte and measures its performance when pure graphite is experimentally evaluated as the carbon source as the operating temperature is varied from 650 to 950 °C. The results are described by fundamental mechanisms of fuel cells that involve activation, ohmic and fuel concentration, or transport loss. In addition, the

* Corresponding author. Tel.: +82 51 510 7330; fax: +82 51 512 5236.
E-mail addresses: kjfeel@pusan.ac.kr (J.-P. Kim), eneryentias@pusan.ac.kr (H. Lim), chjeon@pusan.ac.kr (C.-H. Jeon), changyj@pusan.ac.kr (Y.-J. Chang), koh@pusan.ac.kr (K.-N. Koh), smchoi@kicet.re.kr (S.-M. Choi), jxs704@pusan.ac.kr (J.-H. Song).

0378-7753/$ – see front matter © 2010 Elsevier B.V. All rights reserved.
doi:10.1016/j.jpowsour.2010.05.065

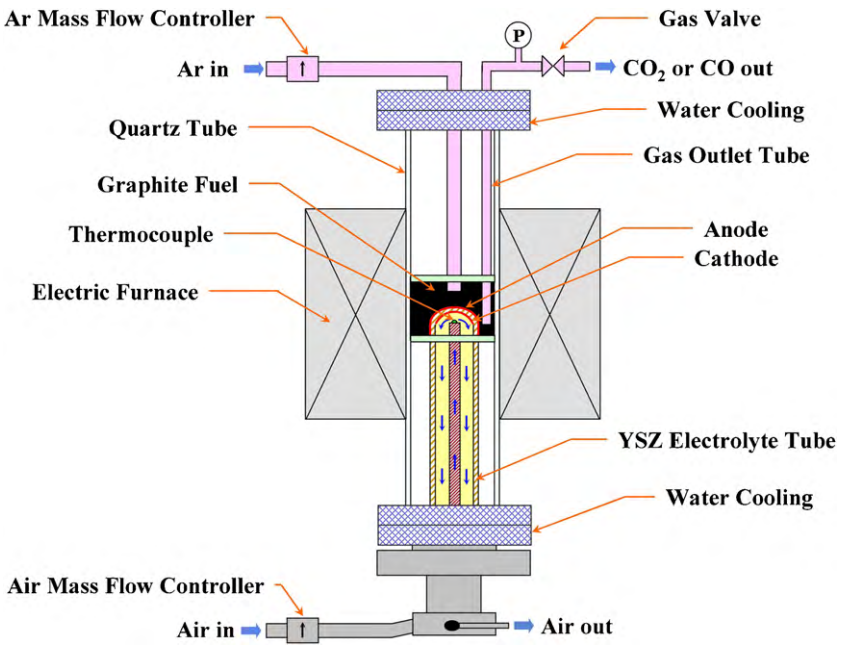

Fig. 1. Schematic of tubular DCFC system.

influence of particle size and feeding conditions on cell performance is thoroughly examined.

2. Experimental

A schematic of the experimental setup of the tubular DCFC system is given in Fig. 1. The single cell consists of a yttria-stabilized zirconia (YSZ) electrolyte tube, and an anode and a cathode each of porous platinum (Pt). The length, outside diameter and thickness of the YSZ electrolyte tube are 300, 10, and 1.5 mm, respectively, and the reaction area of the cell is limited to about 1.57 cm^2. The single cell has a fixed-bed configuration of carbon physically detached from the anode surface and is heated electrically at 5 °C per minute to the desired operating temperature by means of an electric furnace with a maximum temperature of 1000 °C. The inner temperature of the cell is monitored by a thermocouple embedded at the edge of the tubular cell.

Argon gas (purity 99.999 vol.%) at a flow rate of 400 standard cubic centimeters per minute (sccm) was introduced from the top inlet on the anode side to push out product gases such as CO_2 and carbon monoxide (CO) through the gas outlet tube. At certain positions from the outlet, a gas analyzer was used to measure the concentrations of the product gases, which were then compared with theoretical values predicted by a thermodynamic analysis of the chemical equilibrium. The pressure of the cell was measured by a pressure gauge since the relative amounts of flue gas composition are important for determining the rate-controlling reaction among the anode reactions (Section 3.2). Oxygen gas with two different oxygen fractions at a flow rate of 400 sccm was introduced through the inner channel on the cathode side of the tubular cell where oxygen content is consumed on the cathode layer by the electrochemical reaction. Oxygen gas flows regulated controlled by mass flow controllers.

Table 1
Elemental specifications of graphite sample.

Graphite	C	H	S	N
(wt.%)	99.12	0.81	0.06	0.00

Particle sizes of graphite powder considered as fuel were in three groups with ranges of 0–32, 90–150, and 150–180 μm. Scanning electron microscope (SEM) images of the graphite powder are shown in Fig. 2 and elemental specifications of the fuel are listed in Table 1. Wires from the cell are connected to a *I–V* measurement equipment (Model IT8511, DC Electronic Load), which is used to measure the cell performance under load that varied from 0 to 100 mA.

3. Results and discussion

3.1. Cathode reaction mechanism

High-temperature fuel cells, such as a DCFC, typically consist of an oxygen ion electrolyte, electrodes, and electric contacts [19]. The solid electrolyte is coated on both sides with porous electrode materials [12]. Oxygen is incorporated into the electrolyte on the

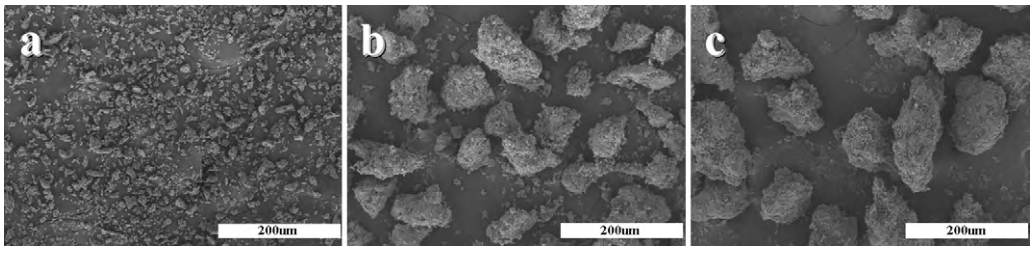

Fig. 2. SEM images of graphite powder: (a) below 32 μm, (b) 90–150 μm, and (c) 150–180 μm.

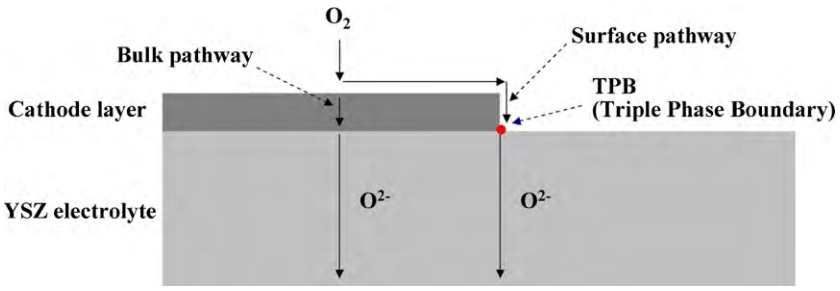

Fig. 3. Schematic representation of possible oxygen reduction pathways at cathode.

cathode side and then diffuses in the form of ions through the electrolyte layer to react with fuel on the anode side. An understanding of the surface chemical reaction at the cathode|electrolyte interface is thus needed to achieve more efficient performance of the cathode. In general, the triple-phase boundary (TPB) region, where the electrolyte, a gas and an electrode meet, is the appropriate place where the oxygen reduction takes place [20].

A schematic representation of the possible oxygen reduction pathways is shown in Fig. 3. Parallel and competing bulk and surface pathways can be observed. One pathway may be dominant or both pathways may be important, with the overall kinetics of the reaction determined by the dominant path [21]. Oxygen reduction involves several mechanisms such as adsorption, dissociation, surface diffusion, bulk diffusion, and charge transfer.

In the present DCFC fuelled by solid graphite, the cathode layer is a porous platinum paste and kinetic losses due to bulk diffusion are reduced by minimizing the cathode layer thickness.

3.2. Anode reaction mechanism

In the present DCFC system, YSZ is the solid oxide electrolyte for the electrochemical oxidation of carbon. A schematic representation of the anode reaction mechanisms is given in Fig. 4. The anode reactions are as follows [22,23]:

$$C + 2O^{2-} \rightarrow CO_2 + 4e^- \quad (1)$$

$$C + O^{2-} \rightarrow CO + 2e^- \quad (2)$$

$$CO + O^{2-} \rightarrow CO_2 + 2e^- \quad (3)$$

These equations indicate that the ideal anode reaction is the electrochemical reaction producing CO_2 (a four-electron process) expressed by Eq. (1), although the formation of CO (a two-electron process) expressed by Eq. (2) may also occur. The generated gaseous CO may react further with oxygen ions at the surface to produce CO_2 via the reaction route given by Eq. (3).

The following Boudouard reaction is a non-electrochemical carbon reaction, which may lower actual efficiency and the open-circuit voltage (OCV) compared with a case where this reaction does not occur [7,15]:

$$C + CO_2 \rightarrow 2CO \quad (4)$$

O^{2-} ions are produced at the cathode via the following reduction reactions:

$$O_2 + 4e^- \rightarrow 2O^{2-} \quad (5)$$

$$O_2 + 2e^- \rightarrow O^{2-} \quad (6)$$

In a subsequent analysis to predict theoretically the maximum cell voltage, further oxidation of the product CO in the anode given by Eq. (3) is ignored and the anode reactions depicted expressed by Eqs. (1) and (2) are thus simplified to a single reaction pathway. In other words, the two reactions are combined into a single reaction using the CO_2 fraction in the product gas, ψ, which varies with temperature and which has been experimentally determined during the reaction of carbon with oxygen [25]. Under this single reaction, the OCV values are calculated over a wider temperature range from the Nernst equation, whose first term involves requires the change of Gibbs free energy at standard pressure [26]. In the Nernst equation, a second logarithmic term expressed in terms of actual pressures of reactants and products is shown to be much smaller than the first term under normal operating conditions at which the partial pressure of the oxygen reactant is observed to be higher than that of the products.

3.3. Effect of temperature and current

The present DCFC uses a solid ceramic electrolyte such as YSZ and operates at temperatures up to 1000 °C. The cell performance is expected to be very sensitive to the operating temperature since elevated temperatures assure higher ion conductivity [13,24].

Calculated maximum cell voltage (OCV) values have been compared with experimental values as operating temperatures were varied from 650 to 950 °C, as illustrated in Fig. 5. Both calculated and experimental OCV values exhibit a gradual increase as the operating temperature is elevated. The experimental values, however, are consistently less than the calculated values because of irreversibilities (alternatively known as 'polarizations'). These differences are losses (such as activation and fuel crossover loss, ohmic resistance loss, and mass transport and concentration loss) that indicate how much the actual fuel cell operation deviates from ideal reversible conditions [26]. As seen in Fig. 5, the difference between calculated and experimental values is greatly reduced when the operating

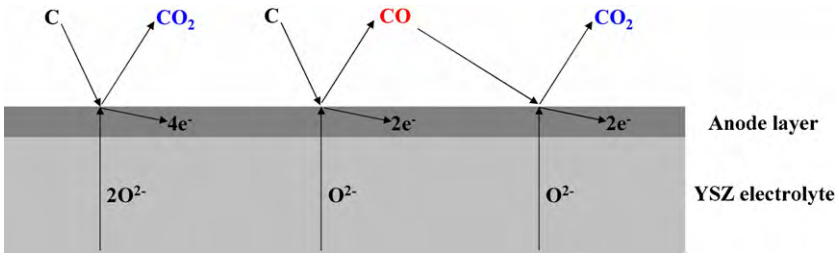

Fig. 4. Schematic representation of carbon reaction mechanisms at anode.

Table 2
Experimental performance values of proposed cell.

Temperature (°C)	650	700	750	800	850	900	950
Open-circuit voltage (V)	0.983	0.996	1.019	1.047	1.075	1.098	1.115
Maximum power density (mW cm^{-2})	0.7	1.5	2.6	5.9	9.1	12.0	16.8

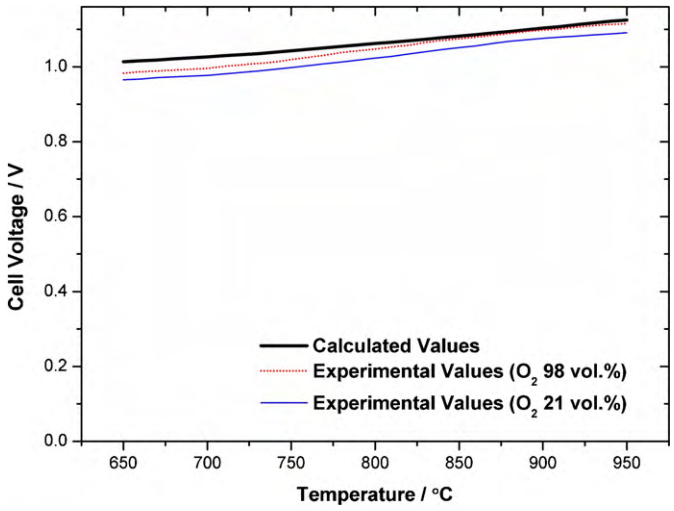

Fig. 5. Comparison of calculated and experimental maximum cell voltage (OCV) values.

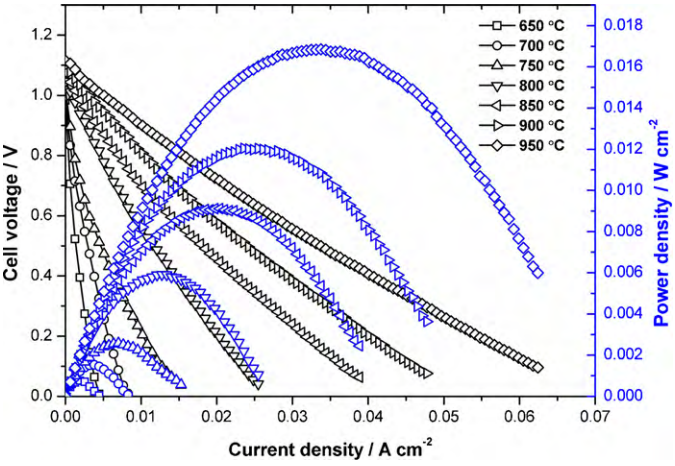

Fig. 6. Effects of temperature and current on actual cell voltage and power density using graphite powder (<32 μm) at oxygen and argon flow rates of 400 sccm.

temperature is elevated. This behaviour is due to minimal activation polarization at high temperatures indicated by the absence of sharp fall-off behaviour near zero current. Also, higher oxygen concentrations on the cathode side combined with higher temperature can produce an OCV close to the theoretical limit due to a similar contribution to the reaction activation process during the early stage.

The cell voltage and the power density (Fig. 6) are affected by temperature and current at oxygen and argon flow rates of 400 sccm when graphite powder below 32 μm is used. Cell voltage and power density are measured as current is increased at temperatures of 650–950 °C at 50 °C intervals. Results show that the cell voltage increases with temperature and linearly decreases with an increase in current density at a constant operating temperature. Experimental performance values of the cell with respect to temperature are listed in Table 2. Elevated temperatures lead to an increase in both maximum power density and current density.

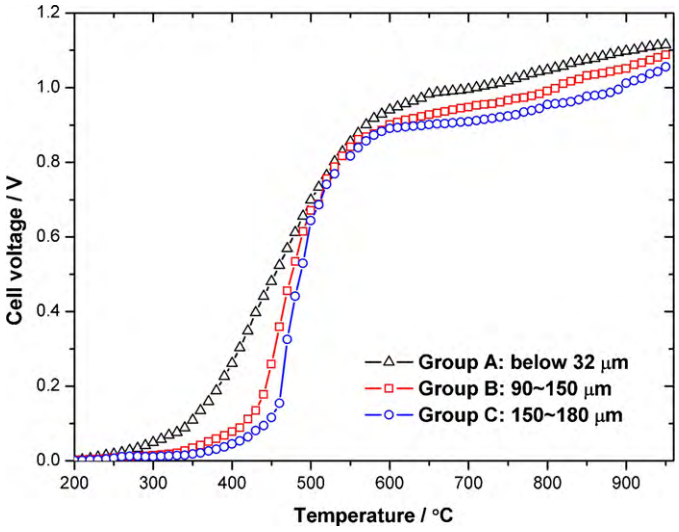

Fig. 7. Effect of varying graphite powder size (below 32, 90–150, and 150–180 μm) on maximum cell voltage (OCV).

These results suggest that ohmic resistance loss is dominant during intermediate current demand, which then decreases with elevated temperature. The absence of a sharp decrease in the heavy load (high current) range may indicate that even at the highest temperature (950 °C) sufficient amounts of reactant are left and prevent any mass transport involvement and concentration loss.

The present DCFC uses platinum as the anode which inevitably limits the OCV to a low current density. Similarly, Gür and Huggins [27] studied a fuel cell for the direct electrochemical conversion of carbon and measured and the OCV of about 1.5 V with a current density of approx. 33 mA cm^{-2} at 955 °C. Horita et al. [28] used a fuel cell that comprised a YSZ electrolyte tube and a porous Pt cathode and reported an OCV of 1.113 and 0.85 V with Ar and CO_2, respectively, flowing through the fixed bed.

3.4. Effect of particle size

Pulverized carbon material is used as fuel for the proposed DCFC. Thus, it is necessary to investigate the size effect of carbon as it electrochemically reacts with oxygen ions and electrons on the anode surface.

The effect of three classes of graphite powder size on the OCV without current imposed is shown in Fig. 7. Cell voltages were measured when the temperature was increased from 200 to 950 °C. When particle sizes are varied in the ranges of 0–32, 90–150, and 150–180 μm at 950 °C, the OCVs are 1.115, 1.088 and 1.056 V, respectively. As the particle size of the graphite powder becomes smaller, the performance greatly improves because the anodic active surface area in contact with, and subsequently reacting with, the carbon particles expands and activation loss on the surface of the anode may therefore be reduced [25].

The effect of graphite size on the OCV becomes more prevalent in the temperature region below 500 °C where electrochemical reactions are kinetically controlled to overcome a reaction-initiating thermal barrier. This again supports the observation that reactions with smaller particles lead to reduced activation loss and thus a relatively higher OCV. Increased surface area resulting from smaller

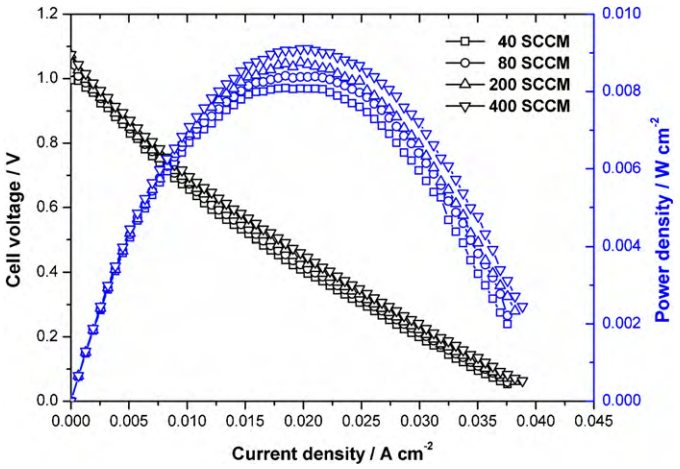

Fig. 8. Effect of argon gas flow rate on cell voltage and power density at 850 °C.

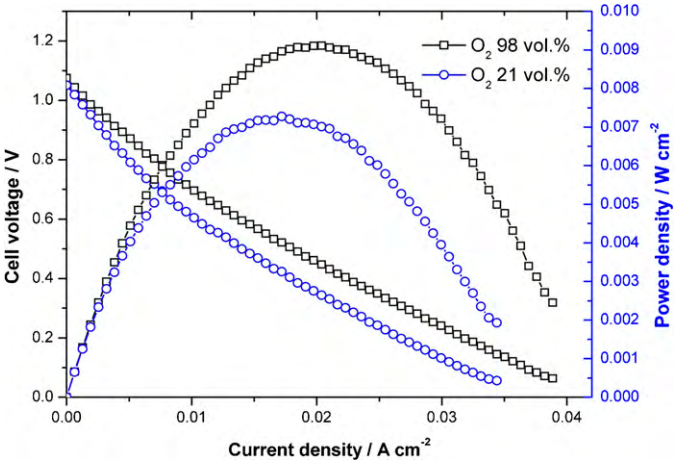

Fig. 9. Effect of oxygen fraction on cell voltage and power density at an oxygen flow rate of 400 sccm at 850 °C.

particles may limit maximum current density due to a higher area specific resistance [14], which is not evaluated here.

3.5. Effect of particle feeding system

Argon is introduced as a carrier gas to deliver the graphite powder for the entrained bed configuration (not employed here) and to push away product gases such as CO_2 and CO from the reacting surface, as mentioned above in Section 2.

The effect of the flow rate of carrier gas in the anode channel on the cell performance at 850 °C with oxygen constant at 400 sccm is shown in Fig. 8. The peak power density of the cell increases by approx. 12.6% from 8.09 to 9.11 mW cm^{-2} as the carrier gas flow rate increases ten times from 40 to 400 sccm. These results imply that the introduction of large amounts of fresh argon minimizes mass transport losses and improves cell performance by reducing the concentrations of product gases which suppress anode reactions on the anodic surface [25].

3.6. Effect of oxygen flow conditions

Air, which is mainly composed of 78.08 vol.% nitrogen, 20.95 vol.% oxygen, 0.93 vol.% argon, 0.03 vol.% carbon dioxide and trace amount of other gases, is generally used for the operation of a fuel cell. Fuel cells can, however, use only about 21 vol.% oxygen. Therefore, it is useful to measure the cell voltage of the present

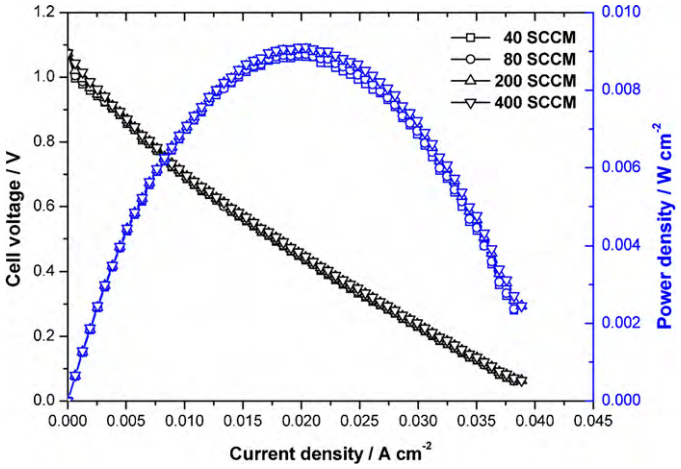

Fig. 10. Effect of oxygen flow rate on cell voltage with oxygen content of 98 vol.% at 850 °C.

DCFC when the oxygen fraction is varied. The maximum cell voltage (OCV) is significantly increased with 98 vol.% oxygen compared to 21 vol.% oxygen, the effect becomes more prevalent at elevated temperatures (Fig. 5). This behaviour can be estimated theoretically from the Nernst equation by considering the sign of second terms, which include the partial pressure ratios of reaction species [25].

The peak power density of the cell with 98 vol.% oxygen increases by about 30% when compared with that of 21 vol.% oxygen, as shown in Fig. 9. These observations indicate that greater availability of transported oxygen ions in the cathode results in faster oxidation of carbon in the anode [26].

As described in Section 2, oxygen and argon are introduced to the cathode channel from the bottom inlet and to the anode channel from the top inlet, respectively. The influence of air flow rate on cell performance is shown in Fig. 10, where oxygen content and argon flow rate are held constant at 98 vol.% and 400 sccm, respectively, at 850 °C. As seen in Fig. 10, the cell performance does not increase appreciably even though the oxygen flow rate increases; this indicates that additional oxygen has no effect when the cathode is already saturated with oxygen.

4. Conclusions

A mechanically simple fuel cell system fuelled by carbonaceous graphite powder is fabricated to produce electricity. Experimental analyses are carried out to evaluate cell performance. The following results are obtained.

(1) In experimental verification of the cell, a maximum OCV of 1.115 V and a power density of 16.8 mW cm^{-2} are achieved at 950 °C. Raising the operating temperature from 650 to 950 °C significantly improves the cell performance.
(2) Calculated and experimental maximum cell voltage (OCV) values become identical at high temperature and thereby indicates a smaller activation loss.
(3) The ohmic loss becomes significant for predicting the actual cell voltage, particularly when current increases and temperature decreases.
(4) Performance is improved with smaller graphite particle sizes because of reduced activation loss.
(5) Increase in the flow rate of carrier gas produces a higher OCV as well as peak power density probably due to reduced mass transport loss.
(6) Increase in the oxygen fraction, rather than the oxygen flow rate has a more significant influence on cell performance due

to greater reactant availability and therefore reduced activation loss.

Acknowledgement

This work was supported by a Research Grant from the PNU Pusan Clean Coal Center.

References

[1] BP Statistical Review of World Energy, June 2009, www.bp.com/statisticalreview.
[2] J. Thijssen, Report No. 1008429, EPRI, Palo Alto, CA, 2004.
[3] E. Patton, S. Zecevic, Report No. 1011496, EPRI, Palo Alto, CA, 2005.
[4] E.J. Carlson, Report No. 1013362. EPRI, Palo Alto, CA, 2006.
[5] T.P. Chen, Report No. 1016170, EPRI, Palo Alto, CA, 2008.
[6] D. Cao, Y. Sun, G. Wang, J. Power Sources 167 (2007) 250–257.
[7] Q. Liu, Y. Tian, C. Xia, L. Thompson, B. Liang, Y. Li, J. Power Sources 185 (2008) 1022–1029.
[8] S. Zecevic, E.M. Patton, P. Parhami, Carbon 42 (2004) 1983–1993.
[9] M.J. Antal Jr., G.C. Nihous, Ind. Eng. Chem. Res. 47 (2008) 2442–2448.
[10] N.J. Cherepy, R. Krueger, K.J. Fiet, A.F. Jankowski, J.F. Cooper, J. Electrochem. Soc. 152 (2005) A80–A87.
[11] X. Xue, J. Tang, N. Sammes, Y. Du, J. Power Sources 142 (2005) 211–222.
[12] S.A. Hajimolana, M. Soroush, Ind. Eng. Chem. Res. 48 (2009) 6112–6125.
[13] J.F. Cooper, Recent Trends in Fuel Cell Science and Technology, Springer, 2007, pp. 248–266.
[14] G.A. Hackett, J.W. Zondlo, R. Svensson, J. Power Sources 168 (2007) 111–118.
[15] S.L. Jain, Y. Nabae, B.J. Lakeman, K.D. Pointon, J.T.S. Irvine, Solid State Ionics 179 (2008) 1417–1421.
[16] R. Liu, C. Zhao, J. Li, F. Zeng, S. Wang, T. Wen, Z. Wen, J. Power Sources 195 (2009) 480–482.
[17] X.Y. Zhao, Q. Yao, S.Q. Li, N.S. Cai, J. Power Sources 179 (2008) 104–111.
[18] A.C. Lee, R.E. Mitchell, T.M. Gür, J. Power Sources 194 (2009) 774–785.
[19] M.B. Ricoult, Solid State Sci. 10 (2008) 670–688.
[20] D. Beckel, A. Bieberle-Hutter, A. Infortuna, U.P. Muecke, M. Prestat, J.L.M. Rupp, L.J. Gauckler, J. Power Sources 173 (2007) 325–345.
[21] V. Lawlor, S. Griesser, G. Buchinger, A.G. Olabi, S. Cordiner, D. Meissner, J. Power Sources 193 (2009) 387–399.
[22] M. Ihara, S. Hasegawa, J. Electrochem. Soc. 153 (2006) A1544–A1546.
[23] S. Hasegawa, M. Ihara, J. Electrochem. Soc. 155 (2008) B58–B63.
[24] S. Srinivasan, Fuel Cells from Fundamentals to Applications, Springer, 2006, pp. 528-529.
[25] D. Vamvuka, E.T. Woodburn, Int. J. Energy Res. 22 (1998) 657–670.
[26] J. Larminie, A. Dicks, Fuel Cell Systems Explained, 2nd ed., John Wiley & Sons, 2003, pp. 25-66.
[27] T.M. Gür, R.A. Huggins, J. Electrochem. Soc. 139 (1992) L95–L97.
[28] T. Horita, N. Sakai, T. Kawada, H. Yokokawa, M. Dokiya, J. Electrochem. Soc. 142 (1995) 2621–2624.